Performance Evaluation of Linear Turbo Receivers Using Analytical Extrinsic Information Transfer Functions

César Hermosilla

Department of Electronic Engineering, Technical University Federico Santa María, Valparaíso 239-0123, Chile
Email: hermosil@inrs-emt.uquebec.ca

Leszek Szczeciński

Institut National de la Recherche Scientifique-Énergie, Matériaux,et Télécommunications, Université du Québec Montreal,
Quebec, Canada J3X 1S2
Email: leszek@inrs-emt.uquebec.ca

Turbo receivers reduce the effect of the interference-limited propagation channels through the iterative exchange of information between the front-end receiver and the channel decoder. Such an iterative (turbo) process is difficult to describe in a closed form so the performance evaluation is often done by means of extensive numerical simulations. Analytical methods for performance evaluation have also been proposed in the literature, based on Gaussian approximation of the output of the linear signal combiner. In this paper, we propose to use mutual information to parameterize the logarithmic-likelihood ratios (LLRs) at the input/output of the decoder, casting our approach into the framework of extrinsic information transfer (EXIT) analysis. We find the EXIT functions of the front-end (FE) receiver analytically, that is, using solely the information about the channel state. This is done, decomposing the FE receiver into elementary blocks described independently. Our method gives an insight into the principle of functioning of the linear turbo receivers, allows for an accurate calculation of the expected bit error rate in each iteration, and is more flexible than the one previously used in the literature, allowing us to analyze the performance for various FE structures. We compare the proposed analytical method with the results of simulated data transmission in case of multiple antennas transceivers.

Keywords and phrases: iterative receivers, turbo processing, performance analysis, MIMO systems.

1. INTRODUCTION

The iterative processing based on the so-called turbo principle, introduced to decode the parallel-concatenated codes (turbo codes) [1], was shown to be a powerful tool approaching the limit of globally optimal receivers. In serially concatenated coding schemes, where the propagation channel is the inner code of rate one, the turbo principle has been used in the problem of temporal equalization [2, 3], spatial separation in multiple-input multiple-output (MIMO) receivers [4, 5], and multiuser detection (MUD) [6, 7, 8].

In the above-mentioned serial concatenation schemes, a generic turbo receiver (T-RX) is composed of a soft-input soft-output (SISO) front-end (FE) receiver and a SISO channel decoder. Both devices, exchanging information using logarithmic-likelihood ratios (LLRs) defined for the coded bits, are separated by the mandatory (de)interleaver whose role is to decorrelate the LLRs. The optimal calculation of LLRs in the FE receiver may be computationally demanding

for high-dimensional systems so, suboptimal but simple, linear T-RXs, that is, the receivers with linear FE, were proposed in the literature [5, 8, 9, 10]. The FE in such case is composed of a linear combiner (LC) whose role is to carry out soft interference cancelling, extract the useful signal and, possibly, suppress the residual interference. The output of the LC is transformed into LLRs by a nonlinear demapper, which depends on the employed modulation.

The general tool to analyze the behavior of turbo receivers/decoders is based on the so-called density evolution (DE) [7, 11], where the LLRs are treated as random variables and changes in their probability density functions (pdfs) (which have to be estimated by means of numerical simulations) characterize the behavior of the iterative process. This computationally demanding approach is often replaced by parametrization of the signal involved in the turbo process in which the SISO devices making up the T-RX are disconnected and each of them is characterized by a *transfer function* relating the input's and the output's parameters. For long

data blocks and perfect interleaving, the input-output relationships defined by the transfer functions are assumed to be maintained even after the devices are reconnected to form the working T-RX [3, 12, 13]. The choice of the appropriate parameter to characterize the signals, affects the quality of the analysis. The mutual information (MI) between the bits and their LLRs was proposed in [3, 12] as a parameter robust with respect to variations of the LLR's pdf [14].

The analytical methods proposed in the literature to analyze the T-RXs, employ signal variance [6, 7] to parameterize the LC's output, assumed Gaussian. Here, we propose to parameterize LLRs at the decoder's input, without making any explicit assumption about their distribution. As a robust parameter, we use mutual information between bits and their LLRs, which casts our method into the framework of the extrinsic information transfer (EXIT) analysis. To obtain the EXIT function of the linear FE analytically, that is, using solely the information about the channel state (and *without simulations* of the actual data transmission), we calculate transfer functions of elementary devices the FE receiver is composed of. This is the main contribution of the paper because such decompositions, although explicit in the T-RX's structure, have not yet been used for analytical purposes. Our technique gives a useful insight into principle of functioning of the linear T-RX (thus may be used to design it), and also, allows us to evaluate its performance in terms of the BER for each iteration. Our approach is more flexible than the one presented in [6, 7] because it can handle changes in the structure of the FE receiver without carrying out additional simulations. The flexibility of our technique is evident when the LLRs passed to the decoder are obtained from multiple-output FE receivers.

The analysis we present is exact for long data blocks with perfect interleaving and in large systems, that is, asymptotically exact for significant number of interfering users in the MUD problem [7], or a significant number of transmit antennas in MIMO reception. However, through the numerical examples, we show that the results obtained are still reasonable for systems with modest dimensions.

The paper is organized as follows. Section 2 defines the system model and introduces the linear FE receivers under study. In Section 3 the principles of the EXIT analysis are outlined and we explain how to obtain the *analytical* EXIT functions for a given channel state. In Section 5 the steps that have to be followed to evaluate the performance of a T-RX are presented, as well as numerical examples showing analytical EXIT charts we obtained. Moreover, through simulations, we demonstrate that the proposed method allows us to evaluate exactly the performance of T-RXs measured in terms of coded BER. We conclude the work in Section 6 commenting on the application of the proposed methods and on its limitations, we evaluate its complexity, and suggest further development venues.

2. SYSTEM MODEL

For the purpose of this paper we consider a baseband, discrete-time, linear model of a multiple-input multiple-output (MIMO) communication system

$$\mathbf{r}(n) = \mathbf{H}\mathbf{s}(n) + \boldsymbol{\eta}(n) \qquad (1)$$

in which the vector $\mathbf{s}(n) = [s_1(n), \ldots, s_M(n)]^{\mathrm{T}}$ is sent at time $n = 1, \ldots, L$ through the $N \times M$ channel matrix $\mathbf{H}$, whose entries are channels' gains between transmit and receive antennas [15]. The observation vector $\mathbf{r}(n) = [r_1(n), \ldots, r_N(n)]^{\mathrm{T}}$ is corrupted by a zero-mean spatially decorrelated white Gaussian noise vector $\boldsymbol{\eta}(n)$ with a covariance matrix $\mathrm{E}\{\boldsymbol{\eta}(n)\boldsymbol{\eta}^{\mathrm{H}}(n)\} = \mathbf{I}_N N_0$, where N_0 is the power spectral density of the noise. The operators $(\cdot)^{\mathrm{T}}$ and $(\cdot)^{\mathrm{H}}$ denote, respectively, the transpose and the conjugate transpose; $\mathbf{I}_N$ is the $N \times N$ unitary matrix and we use $\mathbf{I}_N \equiv \mathbf{I}$ when it does not lead to confusion.

Symbols $s_k(n)$ are obtained via memoryless modulation, that is, mapping codewords $\mathbf{c}_k(n) = [c_{k,1}(n), \ldots, c_{k,B}(n)]$ onto a constellation alphabet $\mathcal{A} = \{\alpha_i : i = 1 : 2^B\}$, $s_k(n) = \mathfrak{M}[\mathbf{c}_k(n)]$. Single-outer-code MIMO systems [4, 16, 17], depicted in Figure 1a, are well suited for the illustration of the proposed method, hence, $c_{k,l}(n) = c(B(nM + k) + l - (M + 1)B)$, $k = 1, \ldots, M$, $l = 1, \ldots, B$, where the coded bits $c(m)$ are obtained from the information bits $\{x(q)\}_{q=1}^{Q}$ using a code $\mathcal{C}[\cdot]$ of rate ρ, and an interleaver $\Pi[\cdot]$:

$$\{c(m)\}_{m=1}^{L \cdot M \cdot B} = \Pi\Big[\mathcal{C}\Big[\{x(q)\}_{q=1}^{Q}\Big]\Big]. \qquad (2)$$

Perfect interleaver $\Pi[\cdot]$ allows us to assume that bits $c_{k,l}(n)$ are independent for all k, l, n [12], and are equiprobably drawn from the set $\{0, 1\}$. Consequently, the symbols $s_k(n)$ are independent and equiprobable. The constellation $\mathcal{A}$ has zero mean, $\sum_{i=1}^{2^B} \alpha_i = 0$, and is normalized, $2^{-B} \sum_{i=1}^{2^B} |\alpha_i|^2 = 1$. For simplicity we assume that the raw spectral efficiency B (the number of coded bits per symbol), and the constellation $\mathcal{A}$ remain unchanged for all data substreams. The numerical results presented in this paper are obtained for $\mathcal{A}$ taken as binary phase shift keying (BPSK), quaternary PSK (QPSK), 8PSK, and 16 quadrature amplitude modulation (16QAM), using Gray mapping [18, Chapter 4.3]. In addition, we consider the mapping (called herein anti-Gray[1]), shown in [20],[2] optimized for the purpose of turbo demapping.

All the elements in (1) can be complex but in the case of real constellation $\mathcal{A}$ (e.g., BPSK), it is convenient to replace the matrix $\mathbf{H}$ by $\mathbf{H}' = [\mathfrak{R}[\mathbf{H}]; \mathfrak{I}[\mathbf{H}]]$, and $\mathbf{I}_N N_0$ by $1/2 \mathbf{I}_{2N} N_0$, where $\mathfrak{R}[\cdot]$ and $\mathfrak{I}[\cdot]$ denote the real and the imaginary part, and $[\cdot; \cdot]$ denotes a vertical concatenation of matrices. Then, all the elements in (1) are real.

We assume that the channel state, denoted by the pair $(\mathbf{H}, N_0)$, is perfectly known.

The presented system model, as well as the method introduced in the paper, may be easily generalized to the problem of turbo multiuser detection [8] or turbo equalization [3].

---

[1]Note that, in fact, term *anti-Gray* may have a different meaning when used with 8PSK; see, for example, [19].

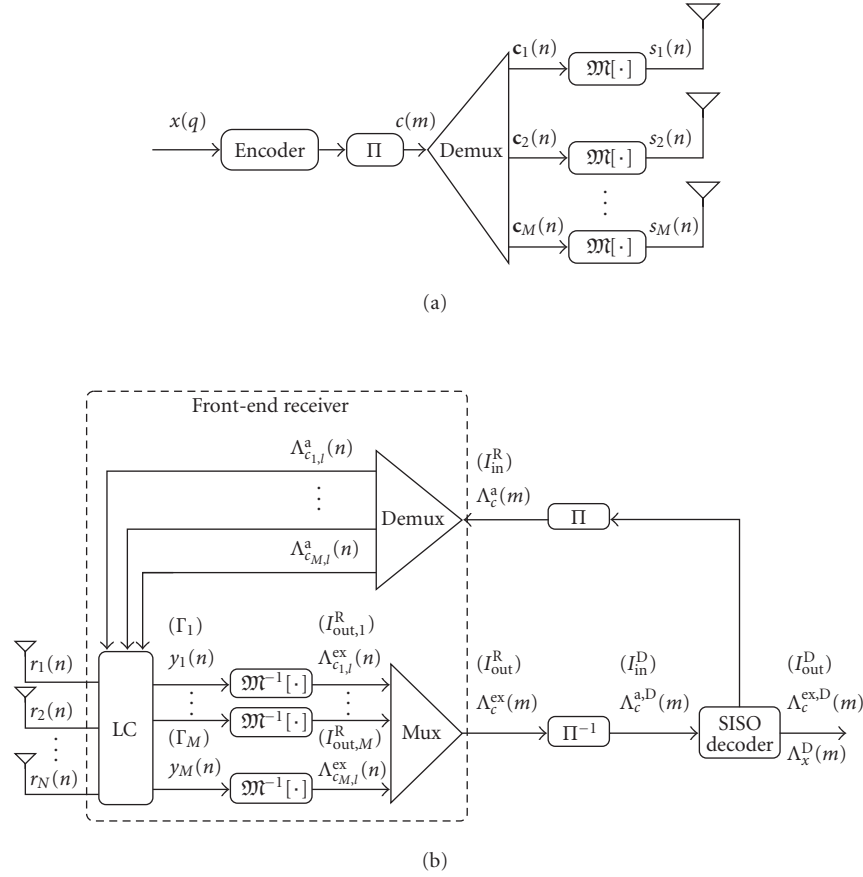[2]For 16QAM, we use $M16^a$ mapping from [20].

(a)

(b)

FIGURE 1: Baseband model of the communications system under consideration: (a) MIMO transmitter with single outer code and (b) turbo receiver; parameters used to characterize the signals are shown in parenthesis.

2.1. Turbo receiver

The turbo receiver is composed of a SISO FE receiver and a SISO decoder exchanging information under the form of LLRs defined for the bit $c_{k,l}(n)$:

$$\Lambda_{c_{k,l}}(n) = \ln \frac{P(c_{k,l}(n) = 1)}{P(c_{k,l}(n) = 0)}, \qquad (3)$$

where $P(\cdot)$ denotes probability.

The SISO decoder, is implemented here with the MAP algorithm [21, 22]. It produces an extrinsic LLR $\Lambda_{c_{k,l}}^{ex,D}(n)$ for the coded bits $c_{k,l}(n)$, given the input (a priori) LLRs $\Lambda_{c_{k,l}}^{a,D}(n)$. The obtained extrinsic LLRs are used as a priori information by the FE receiver in the subsequent iteration. The decoder also delivers the LLRs corresponding to the information bits $\Lambda_x^D(q)$, which are the final product of the T-RX, since the sign of $\Lambda_x^D(q)$ determines the estimate of the bit $x(q)$.

The SISO front-end (FE) receiver, considered here, is composed of a linear combiner (LC) operating on the received data $\mathbf{r}(n)$, and of a nonlinear demapper $\mathfrak{M}^{-1}[\cdot]$, transforming the output of the first one into the LLRs (cf. Figure 1b).

The LC carries out soft interference cancellation followed by signal combining [3, 5, 8, 9, 10, 23]:

$$\begin{aligned} \mathbf{r}_k'(n) &= \mathbf{r}(n) - \left[\mathbf{H}E\{\mathbf{s}(n)\} - \mathbf{h}_k E\{s_k(n)\} \right], \\ y_k(n) &= \mathbf{w}_k^H(n)\mathbf{r}_k'(n), \end{aligned} \qquad (4)$$

where $\mathbf{h}_k$ is the kth column of matrix $\mathbf{H}$ and expectation $E\{\cdot\}$ is calculated using a priori LLRs $\Lambda_{c_{k,l}}^a$ [10].

In the following we consider only time-invariant receivers, that is, $\mathbf{w}_k(n) \equiv \mathbf{w}_k$, although in general the combiner weight may vary in time [8, 10, 23]. The combining vectors $\mathbf{w}_k$ depend on how the FE receiver exploits the information about the interferers. Two types of FE receivers are analyzed here.

(i) T-MRC receiver. *Turbo* maximum ratio combining employs $\mathbf{w}_k = \mathbf{h}_k$, that is, a matched filter [24] which is optimal only in absence of interference.

(ii) T-MMSE receiver. This time-invariant (simplified) version of the optimal receiver, minimizing the mean square error between $y_k(n)$ and $s_k(n)$, is given by [10]

$$\mathbf{w}_k = \left(\mathbf{H}\bar{\mathbf{V}}\mathbf{H}^H + (1 - \bar{v}_k)\mathbf{h}_k\mathbf{h}_k^H + \mathbf{I}N_0 \right)^{-1}\mathbf{h}_k, \qquad (5)$$

where $\bar{\mathbf{V}} = \text{diag}(\bar{v}_1, \ldots, \bar{v}_M) = (1/L) \sum_{n=1}^{L} \mathbf{V}(n)$. Matrix $\mathbf{V}(n) = \text{diag}\{v_1(n), \ldots, v_M(n)\}$ contains on its diagonal the symbols' variances $v_k(n)$, $k = 1, \ldots, M$:

$$v_k(n) = v_k\big(\Lambda^{\mathrm{a}}_{c_{k,1}}(n), \ldots, \Lambda^{\mathrm{a}}_{c_{k,B}}(n)\big)$$
$$= \mathrm{E}\big\{|s_k(n)|^2\big\} - |\mathrm{E}\{s_k(n)\}|^2, \tag{6}$$

where we underline the dependence of the symbol's variance on $\Lambda^{\mathrm{a}}_{c_{k,l}}(n)$. Thanks to the variance averaging, the receiver is calculated only once per block and not for every time index n.

To compute the extrinsic LLRs of the coded bits the demapper assumes that $y_k(n)$ is conditionally Gaussian, with mean [8, 10]

$$\mu_k(n) = \mathrm{E}\{y_k(n)|\mathbf{c}_k(n)\} = \mu_k \mathfrak{M}[\mathbf{c}_k(n)], \tag{7}$$

where $\mu_k = \mathbf{w}_k^{\mathrm{H}}\mathbf{h}_k$, and variance

$$\sigma_k^2(n) = \text{Var}\{y_k(n)|\mathbf{c}_k(n)\}$$
$$= \mathbf{w}_k^{\mathrm{H}}\big(\mathbf{H}\mathbf{V}(n)\mathbf{H}^{\mathrm{H}} - v_k(n)\mathbf{h}_k\mathbf{h}_k^{\mathrm{H}} + \mathbf{I}N_0\big)\mathbf{w}_k. \tag{8}$$

Then, the extrinsic LLRs are given by [3, 8]

$$\Lambda^{\mathrm{ex}}_{c_{k,l}}(n) = \ln \frac{\sum_{\mathbf{b} \in \mathcal{B}_{[l,1]}} \exp\left(-|\mu_k \mathsf{M}[\mathbf{b}] - y_k(n)|^2/\sigma_k^2(n) + \sum_{j=1,\,j\neq l}^{B} b_j \Lambda^{\mathrm{a}}_{c_{k,j}}(n)\right)}{\sum_{\mathbf{b} \in \mathcal{B}_{[l,0]}} \exp\left(-|\mu_k \mathsf{M}[\mathbf{b}] - y_k(n)|^2/\sigma_k^2(n) + \sum_{j=1,\,j\neq l}^{B} b_j \Lambda^{\mathrm{a}}_{c_{k,j}}(n)\right)}, \tag{9}$$

where $\mathcal{B}_{[l,\beta]}$ is the set of all codewords $\mathbf{b} = [b_1, \ldots, b_B]$ having the lth bit b_l set to β.

For BPSK modulation, (9) simplifies to [8, 10]

$$\Lambda^{\mathrm{ex}}_{c_{k,1}}(n) = \frac{2y_k(n)\mu_k}{\sigma_k^2(n)}. \tag{10}$$

Similar simplification may be obtained for QPSK with Gray mapping. For higher-order constellations (e.g., 8PSK, 16QAM), we simplify the computation of (9) using the max-log approximation, that is, $\ln(e^{\lambda_1} + e^{\lambda_2}) \approx \max(\lambda_1, \lambda_2)$ [4].

3. PARAMETRIC DESCRIPTION OF THE ITERATIVE PROCESS

As we already mentioned, the parameterization of the signals simplifies the analysis of the iterative process. Once the appropriate parameters are chosen, the transfer functions of each of the devices must be found. We briefly compare, from the point of view of the flexibility of the resulting analytical tool, the parameterization used in the literature and the one we propose in this paper; we also introduce the notation for the EXIT analysis.

Commonly, the LLRs at the FE receiver's input $\Lambda^{\mathrm{a}}_c(m)$ (and thus at the decoder's output as well, $\Lambda^{\mathrm{ex,D}}_c(m)$) are assumed Gaussian and consistent [3, 7, 12, 13] so, variance is sufficient for their parameterization. We use the same approach in this paper. As for the second signal to be parameterized, the approach proposed in [6, 7] uses the output of the LC $y_k(n)$, assuming it to be Gaussian, so the averaged variance $\bar{\sigma}_k^2 = \mathrm{E}\{\sigma_k^2(n)\}$ is the sufficient parameter to characterize the signal. Then, through simulations, a relationship between $\bar{\sigma}_k^2$ and the variance of LLRs at the decoder's output is established. In this approach the demapper and the decoder are treated, *de facto*, as one device.

If the transfer functions were known for a given channel state $(\mathbf{H}, N_0)$, they might be used to analyze the performance of the T-RX, for example, in terms of information bit error rate, that is, coded BER [6, 7]. The knowledge of transfer functions might also be used to design the transmitter/receiver according to some optimality criterium.

For instance, [19] designs the encoder for the iterative decoding-demapping receiver, having fixed the demapper. Similarly, if the T-RX is used, we might want to adapt the modulation (or coding) for the particular (fixed and known) channel state. Parameterizing the outputs $y_k(n)$ [6, 7], makes such a design difficult because the simulated decoder's transfer function depends, in fact, not only on the decoder itself but also on the demapper, that is, on the modulation employed.[3] Such approach is inflexible because separate simulation would be required for each pair (decoder, demapper), it also hides the impact of each device on the overall performance, limiting the insight one might get into the operation of the T-RX.

Moreover, we note that LLRs passed to the decoder may be obtained from LC with multiple outputs (each with different signal-to-interference- and-noise ratio). This occurs, for example, in a single-outer-code MIMO transmitter [4] (example used in this paper), or when using cyclic space-time interleaver [5]. A similar situation is encountered when combining transmissions in an incremental hybrid ARQ [25]; then, the outputs of FE receiver in different time instances are multiplexed and fed to the same decoder. In such cases, using average variances $\bar{\sigma}_k^2$ is clearly impractical as it would

---

[3] Using analysis [6, 7] when modulations other than BPSK or QPSK with Gray mapping are employed may be done. In such case the decoder's transfer function, beside the variance $\bar{\sigma}_k^2$, must take some parameter of a priori LLRs as the second input.

require a transfer function of the decoder with as many input parameters as there are LCs outputs. Also, as already mentioned, this function would have to be resimulated each time the modulation changes.

To solve this problem, we propose to parameterize the LLR's at the decoder's input, so its transfer function becomes independent of the modulation $\mathfrak{M}[\cdot]$ or the channel structure (matrix $\mathbf{H}$).

We propose to use extrinsic mutual information, casting our approach into the EXIT framework. The EXIT analysis was proposed in [12] to describe the behavior of turbo decoders and later was used in [3] to analyze the convergence of turbo equalizers. In this approach LLRs are parameterized using mutual information (MI) between LLRs $\Lambda(n)$ and the corresponding bits $c(n)$:

$$I(\Lambda; c) = \frac{1}{2} \sum_{b=\{0,1\}} \int_{-\infty}^{\infty} p_{\Lambda|c}(\lambda|b) \log_2 \frac{2 p_{\Lambda|c}(\lambda|b)}{p_{\Lambda|c}(\lambda|1) + p_{\Lambda|c}(\lambda|0)} d\lambda, \tag{11}$$

which was shown to be parameter robust with regard to various forms of pdf's $p_{\Lambda|c}(\lambda|b)$ [14]. Note, that we do not make any explicit assumption about the distribution of the LLRs at the FE's output; we will rather rely on the characteristics of the demapper to obtain the desired MI information value.

To describe the behavior of the turbo process, the SISO FE receiver and the SISO decoder, are characterized by the extrinsic information transfer (EXIT) functions $I_{\text{out}}^{\text{R}} = f^{\text{R}}(I_{\text{in}}^{\text{R}})$ and $I_{\text{out}}^{\text{D}} = f^{\text{D}}(I_{\text{in}}^{\text{D}})$, relating the input MIs, $I_{\text{in}}^{\text{R}} = I(\Lambda_c^{\text{a}}; c)$, $I_{\text{in}}^{\text{D}} = I(\Lambda_c^{\text{D,a}}; c)$ to the output MIs $I_{\text{out}}^{\text{R}} = I(\Lambda_c^{\text{ex}}; c)$, $I_{\text{out}}^{\text{D}} = I(\Lambda_c^{\text{D,ex}}; c)$.

Since the analytical expression relating the decoder's input and output MIs is not available, the function $f^{\text{D}}(\cdot)$ has to be obtained numerically. For this purpose, random data bits $c(n)$ and the corresponding Gaussian LLRs $\Lambda_c^{\text{a}}(n)$ with pdf

$$p_{\Lambda_c^{\text{a}}|c}(\lambda \mid c = b) = \phi(\lambda|b; \sigma_I^2)$$
$$= \frac{1}{\sqrt{2\pi}\sigma_I} \exp\left\{ -\frac{|\lambda - (b - 1/2)\sigma_I^2|^2}{2\sigma_I^2} \right\} \tag{12}$$

are generated [3, 12] and passed through the decoder yielding $\Lambda_c^{\text{D,ex}}(n)$. The latter are used to calculate the output MI (through histograms or via simplifications shown in [19]). From (12) we see that the input MI (I_{in}) depends only on the variance σ_I^2:

$$I_{\text{in}} = I(\Lambda_c^{\text{a}}; c) = f_I(\sigma_I^2), \tag{13}$$

and is found via numerical integration, replacing (12) in (11) [3].

The EXIT analysis is useful for performance evaluation since the relationship between BER after decoding, and the decoder's output MI, that is, BER $= f_{\text{BER}}(I_{\text{out}}^{\text{D}})$, may be established numerically [3] or analytically [12].

We note that, in general, the functions $f_{\text{BER}}(\cdot)$ and $f^{\text{D}}(\cdot)$ are obtained *numerically*. However, because the encoder (and thus the decoder as well) is an invariant element of the transceiver, these functions are calculated only once (offline), and thus may serve for analytical evaluation.[4]

4.   ANALYTICAL EXIT FUNCTIONS

Unlike the encoder, the channel is not a fixed part of the system (e.g., due to fading in wireless transmission) so that the transfer function $f^{\text{R}}(\cdot)$ has to be calculated for each channel state ($\mathbf{H}, N_0$). Using simulation for this purpose would therefore be very time-consuming and the analytical approach proposed in what follows is then a significant advantage. Moreover, we might want to use the EXIT analysis for adaptation of the transmitter structure to the instantaneous channel state; then, the analytical low-complexity approach is a must.

To obtain the function $f^{\text{R}}(\cdot)$, we decompose the FE receiver into elementary devices (a linear combiner and a nonlinear demapper) and describe each of them independently. This allows us to obtain the function $f^{\text{R}}(\cdot)$ if the following assumptions hold.

(A1) The distribution of $\Lambda_c^{\text{a}}(n)$ conditioned on the transmitted bit $c \in \{0, 1\}$ is Gaussian $\phi_{\Lambda_c^{\text{a}}|c}(\lambda \mid c = b) = \phi(\lambda|b; \sigma_I^2)$. Through (13), this "classical" assumption [3, 12] establishes the relationship between σ_I^2 and the receiver's input MI $I_{\text{in}}^{\text{R}} = f_I(\sigma_I^2)$.

(A2) The linear combiner's outputs $y_k(n)$ are decorrelated and Gaussian with expectation $\mu_k(n) = \mu_k s_k(n)$ and variance $\bar{\sigma}_k^2 = \text{E}\{\sigma_k^2(n)\}$. This is equivalent to assuming that $y_k(n)$ is the output of the additive white Gaussian noise (AWGN) channel with the signal-to-interference-and-noise ratio (SINR)

$$\Gamma_k = \frac{|\mu_k|^2}{\bar{\sigma}_k^2}. \tag{14}$$

The expectation applied to the random variable $\sigma_k^2(n)$ in (8) to obtain $\bar{\sigma}_k^2$ expresses the idea that $y_k(n)$ has a *random* pdf which converges to a nonrandom pdf for a sufficiently large M [7].

(A3) The pdf of LLRs at the demapper's output $\Lambda_{c_{k,l}}^{\text{ex}}(n)$ satisfies the consistency conditions [13, 19].

Then, the devices making up the FE depend only on the parameters of the signals being passed and not on the way the latter were generated. To obtain the output MI $I_{\text{out}}^{\text{R}}$ using the input MI I_{in}^{R} and the channel state ($\mathbf{H}, N_0$), we proceed in

---

[4]If the code is allowed to vary, for example, in adaptive modulation/coding, it is chosen from a small number of alternatives [26] so, even then, the offline simulations are feasible.

the following steps:

$$\Gamma_k = F_k(I_{in}^R; \mathbf{H}, N_0), \tag{15}$$

$$I_{out,k}^R = G(\Gamma_k, I_{in}^R), \tag{16}$$

$$I_{out}^R = \frac{1}{M} \sum_{k=1}^{M} I_{out,k}^R, \tag{17}$$

where $F_k(\cdot)$ describes the functional behavior of the LC and $G(\cdot, \cdot)$ characterizes the demapper. Demultiplexing of LLRs taken from the different substreams is modelled as averaging (17), which is possible thanks to assumption (A3). Note, that (A3) is always satisfied if (A2) holds, and if the exact formula (9) is used, that is, having $y_k(n)$ Gaussian makes $\Lambda_{c_{k,l}}^{ex}(n)$ consistent, however, (A3) is needed because we use the max-log approximation of (9).

4.1. Linear combiner

In this subsection we obtain the function $F_k(\cdot)$, describing the relationship between Γ_k, the channel state, and the input MI for a given type of linear receiver (here, T-MMSE or T-MRC). Replacing equations (7) and (8) and the expression for $\mathbf{w}_k$ (depending on the type of receiver) in (14), the dependence of Γ_k on the channel state is explicit. The relationship with the input MI I_{in}^R, however, is not direct since this parameter affects $\bar{\sigma}_k^2$ and $\mathbf{w}_k$ through matrix $\bar{\mathbf{V}} \simeq E\{\mathbf{V}(n)\}$, where we replace the time-averaged symbol variance with expectation assuming ergodicity of the process $\Lambda_{c_{k,l}}^a(n)$.

The variance $v_k(n)$ of the symbol $s_k(n)$, given by (6) depends on the random $\Lambda_c^a(n)$. Due to demultiplexing, the conditional distribution of a priori LLRs $\phi_{\Lambda|c}(\lambda|c; \sigma_I^2)$ is the same for all substreams, thus, the average symbol variances are equal $\bar{v}_k \equiv \bar{v}$. They depend only on σ_I^2 (assumption (A1) relates the input MI I_{in}^R to this parameter) and may be calculated as

$$\bar{v}(\sigma_I^2) = E\{v_k(n)\} = 1 - \sum_{n=1}^{2^B} \sum_{m=1}^{2^B} \alpha_n \alpha_m^* \prod_{l=1}^{B} \Phi(b_{m,l} \oplus b_{n,l}; \sigma_I^2), \tag{18}$$

where $\alpha_m = \mathfrak{M}[\mathbf{b}_m]$, $\oplus$ denotes binary exclusive-or, and the function $\Phi(b; \sigma_I^2)$, $b \in \{0, 1\}$ is defined as

$$\Phi(b; \sigma_I^2) = \frac{1}{2} \int_{-\infty}^{\infty} \frac{e^{\lambda b}}{(1 + e^\lambda)^2} [\phi(\lambda|1; \sigma_I^2) + \phi(\lambda|0; \sigma_I^2)] d\lambda. \tag{19}$$

The details of this derivation are shown in Appendix A.

Since σ_I^2 and I_{in}^R are related, we show in Figure 2 the relationship between $\bar{v}$ and I_{in}^R.

Observe that maintaining the same value of input MI at the FE, the average symbol variance grows if the modulation level increases, which means that the interference is also increased (cf. (8)). The increase is slight for Gray mapping but important for anti-Gray mapping. This may be explained
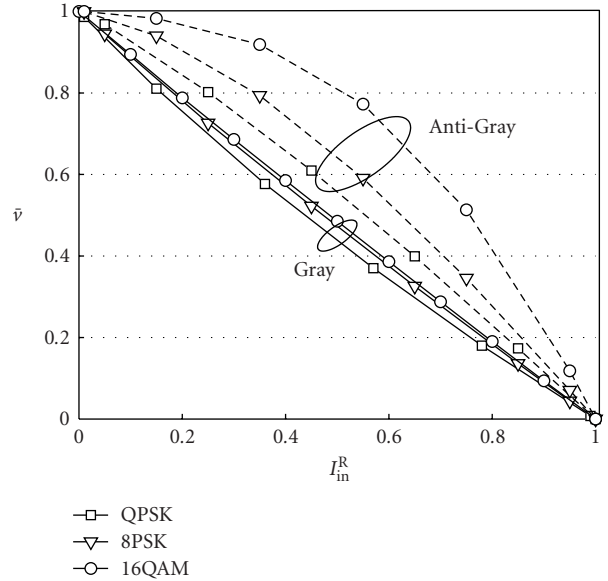

FIGURE 2: Relationship between average symbol variance $\bar{v}$ and a priori MI I_{in}^R for QPSK, 8PSK, and 16QAM modulations with Gray and anti-Gray mappings.

noting that for relatively high MI (e.g., $I_{in} \approx 0.4$) the most likely symbols $\alpha_i = \mathfrak{M}[\mathbf{b}_i]$ are those having the labelling bits $\mathbf{b}_i$ similar (e.g., one-bit change) to $\mathbf{c}_k(n)$, which were actually used to modulate the symbol $s_k(n) = \mathfrak{M}[\mathbf{c}_k(n)]$. By the nature of Gray mapping, changing one bit in $\mathbf{c}_k(n)$ yields modulated symbols geometrically close to the $s_k(n)$ (this translates into low variance). While for anti-Gray mapping, one-bit change corresponds to symbols placed as far apart as possible (in order to maximize the MI when $I_{in}^R = 1$, cf. [20]). This results of course in high value of symbol's variance.

4.2. Nonlinear demapper

For an *arbitrary* modulation $\mathfrak{M}[\cdot]$ and *arbitrary* value of input MI, we may obtain the desired relationship (16) using Monte-Carlo integration in the following manner. First, we generate randomly one stream of bits $c_l(n)$, $l = 1, \ldots, B$ as well as their corresponding a priori LLRs $\Lambda_{c_l}^a(n)$ with Gaussian pdf $\phi(\lambda|c_l(n); \sigma_I^2)$, thus $I_{in}^R = f_I(\sigma_I^2)$. Next, the modulated symbols $s(n) = \mathfrak{M}[c_1(n), \ldots, c_B(n)]$ are passed through the interference-free channel whose output is given by $y(n) = s(n) + \xi(n)$, where $\xi(n) \sim \mathcal{N}(0, 1/\Gamma)$ (assumption (A2)). The extrinsic LLRs for bits $c_l(n)$, obtained from $y(n)$ (9), are then used to calculate the MI. The functions we obtain for QPSK and 16QAM modulations using Gray and anti-Gray mappings are shown in Figure 3. We emphasize that they depend only on the modulation $\mathfrak{M}[\cdot]$ and do not depend on the channel state $(\mathbf{H}, N_0)$ or the linear receiver's $\mathbf{w}_k$. Therefore, despite their numerical origin, they are still useful for analytical evaluation.

We note, that it is possible to obtain the exact analytical form of $G(\cdot, 1)$, that is, for $I_{in}^R = 1$, and, in the case of Gray mapping, we may get a simple approximation of $G(\cdot, 0)$.
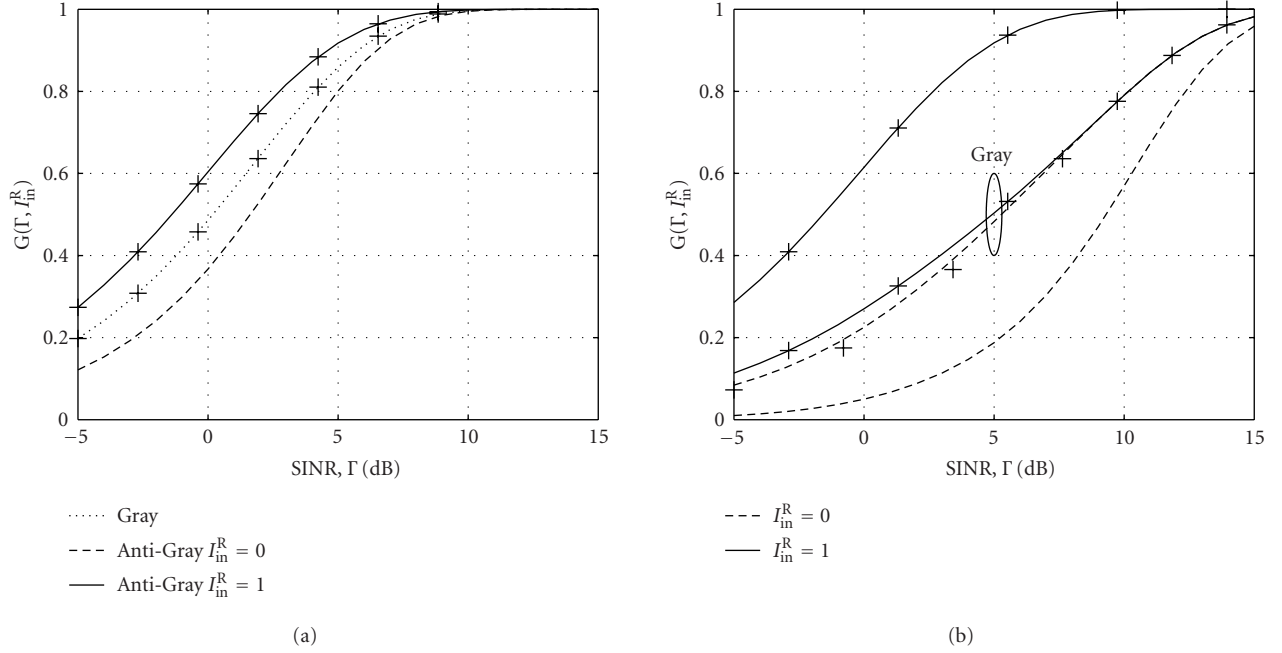
(a)

(b)

FIGURE 3: Functions $G(\Gamma, I_{in}^{R})$ for (a) QPSK and (b) 16QAM modulations with Gray and anti-Gray mappings. Markers correspond to the analytical results obtained using the method explained in Appendix B.

---

(1) Initialization step: $j = 1$; $I_{out}^{D,(0)} = 0$.
(2) Get FE input MIs using decoder's output MI from previous iteration $I_{in}^{R,(j)} = I_{out}^{D,(j-1)}$.
(3) Compute the symbols' average variance $\bar{v}$ using (18); obtain σ_I^2 from inverse relationship (13).
(4) Calculate the receiver $\mathbf{w}_k$ (from (5), in T-MMSE case), and the average variance $\bar{\sigma}_k^2$ from (8); use (14) to obtain Γ_k.
(5) Compute the MIs $I_{out,k}^{R,(j)}$ using (16) and get $I_{out}^{R,(j)}$ via (17).
(6) Obtain the decoder's output MI $I_{out}^{D,(j)} = f^D(I_{out}^{R,(j)})$.
(7) Calculate BER as $\text{BER}^{(j)} = f_{BER}(I_{out}^{D,(j)})$.
(8) Return to step (2) using $j = j + 1$ (next turbo iteration).

ALGORITHM 1: Performance evaluation steps; index (j) denotes the MI values obtained in the jth iteration.

The numerical results presented in Figure 3, are based on derivation of the formulas shown in Appendix B. Although such approach is not sufficient to obtain the function $G(\cdot, I_{in}^{R})$ for any I_{in}^{R}, it is useful to calibrate the numerical procedures for extreme values of MI.

5. PERFORMANCE EVALUATION AND NUMERICAL EXAMPLES

The function $G(\Gamma_k, I_{in}^{R})$ is obtained analytically for the modulations with Gray mapping and by Monte-Carlo integration in other cases, $\bar{v}(\sigma_I^2)$ in (18) is numerically computed off-line. These two nonlinear functional relationships are then stored in the lookup table and interpolated when needed. So, once the channel state $(\mathbf{H}, N_0)$ is known, the EXIT function of the receiver $f^R(\cdot)$ is obtained *without* any simulation, that is, *analytically*. We thus use the word *analytical* with respect to

the procedure for obtaining the function $f^R(\cdot)$ for different channels states and not with regard to the way the nonlinear functional relationships, for example, $f_I(\cdot)$, $\bar{v}(\cdot)$, or $G(\cdot, \cdot)$, were obtained.[5] In the same sense, BER of the T-RX may be found analytically.

In Algorithm 1 we resume the steps which have to be taken to compute BER for a given channel state, $(\mathbf{H}, N_0)$.

Note that interpolations (linear) are necessary for each iteration: 1D interpolations are used in steps (3), (6), and (7), while step (5) requires M 2D interpolations. Because the decoder's output MI I_{out}^D has one-to-one relationship with σ_I^2, only one of these parameters is necessary; this observation saves one 1D interpolation.

---

[5]Note, for example, that the evaluation of the BER in the AWGN channel will still be called analytical, even if it uses the so-called error function [18, Chapter 5.2.1], which is not available analytically.
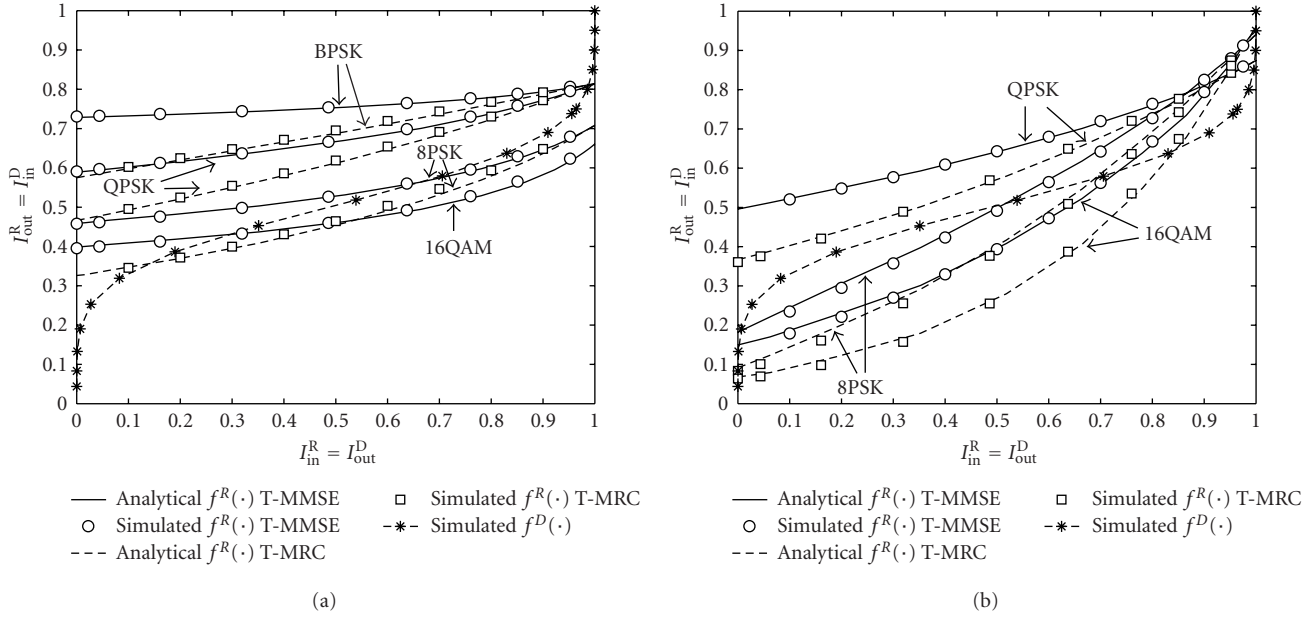
FIGURE 4: EXIT functions of the T-MMSE and T-MRC FE receiver for the channel state $(\mathbf{H}_0, N_0)$ when employing different modulations $\mathfrak{M}[\cdot]$: (a) Gray mapping and (b) anti-Gray mapping. The rate $\rho = 1/2$ decoder's EXIT function is also presented; noise level is normalized so that E_b/N_0 is the same for each modulation.

5.1. EXIT functions

Consider a system with $N = M = 4$ antennas, using a rate $\rho = 1/2$ convolutional code with generator polynomials $\{5, 7\}_8$; $Q = 4000$ information bits are generated in one block $\{x(q)\}_{q=1}^{Q}$; random interleaver $\Pi[\cdot]$ is used.

Figure 4 compares the EXIT functions obtained by simulation and analytically for the receivers T-MMSE and T-MRC with different modulations $\mathfrak{M}[\cdot]$ when the channel is given by

$$\mathbf{H}_0 =$$

$$\begin{bmatrix} 0.36-0.45\imath & 0.71+0.45\imath & 0.67+0.18\imath & 0.93+0.75\imath \\ 0.20+0.21\imath & -0.07-0.88\imath & 0.64+0.95\imath & -0.99-0.65\imath \\ 0.24+0.16\imath & -0.05+0.86\imath & -0.59+0.56\imath & 1.12-0.05\imath \\ -0.62+0.29\imath & -0.36-0.32\imath & -0.51-0.47\imath & 0.63-0.29\imath \end{bmatrix},$$
$$(20)$$

and noise level is normalized, $N_0 = 1.6/B$ so that E_b/N_0,

$$\frac{E_b}{N_0} = \frac{\text{tr}\{\mathbf{H}^H\mathbf{H}\}}{M \cdot N\rho B N_0}, \qquad (21)$$

is the same independently of the employed modulation; here $\text{tr}\{\cdot\}$ denotes the matrix trace.

We may observe a very good match between the analytical and simulated EXIT functions. Our method gives, therefore, a useful insight into the behavior of the iterative process without simulating the EXIT functions. These EXIT charts may be compared to those shown normally in the context of turbo demapping [19]. The difference, however, results from

the presence of the interference-inducing dispersive channel $\mathbf{H}$ so the value of the MI at the FE's output depends on both the channel state and the input MI.

First note, that if $I_{\text{in}}^{R} = 1$, the T-MMSE and T-MRC receivers' EXIT functions coincide for $f^R(1)$. This is natural because, a complete a priori information allows for perfect elimination of the interference in (4) so $\mathbf{w}_k \sim \mathbf{h}_k$ (by putting $v_k = 0$ in (5)). On the other hand, if $I_{\text{in}}^{R} = 0$, receiver T-MMSE normally outperforms receiver T-MRC.[6] Note also, that $f^R(1)$ is the same whether BPSK or QPSK modulation is employed. This is because for perfect interference cancellation, and due to the normalization of the noise level, the SINR in the real/imaginary branch of QPSK is the same as the SINR of BPSK. However, because QPSK's function starts with lower $f^R(0)$ than BPSK, the convergence will occur at a lower value of I_{out}^{D}. As a consequence, the BER figure will be better for BPSK when compared to QPSK. The difference will disappear, though, for high E_b/N_0 when the function $f^R(\cdot)$ moves "up" and flattens. This observation was confirmed by simulations (not shown for limited space).

Analyzing the form of the functions $f^R(\cdot)$ for Gray mapping, we conclude that, even if the starting point $f^R(0)$ decreases when the modulation level grows, the general form is quite similar. This is because the demapper functions are rather insensitive to the value of input MI (cf. Figure 3) and the relationship between the symbols' variance $\bar{v}$ and the input MI is quite similar for all the modulations considered (cf. Figure 2).

---

[6]Both receivers are equivalent if the matrix $\mathbf{H}^H\mathbf{H}$ is diagonal, that is, when the substreams do not interfere with each other.
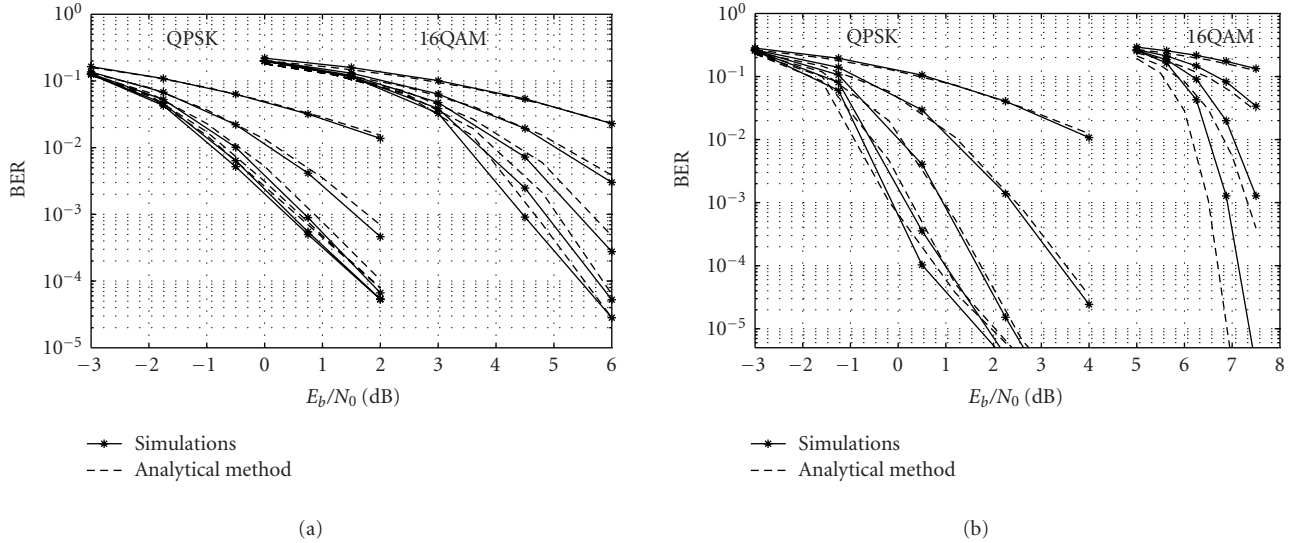
FIGURE 5: Simulated and analytical BER obtained by means of T-MMSE receivers for the channel $\mathbf{H}_0$: (a) Gray mapping and (b) anti-Gray mapping.

The situation changes significantly in the case of anti-Gray mapping. Although the relationship between the starting point $f^R(0)$ and the input MI is the same as in the Gray mapping, it is inverted for the final point $f^R(1)$, that is, 16QAM provides higher MI than that of 4QAM (cf. Figure 3). This is due to the constellation mapping designed so as to maximize demapper's output MI when $I_{in}^R = 1$ [20]. We note also, that the EXIT function obtained with 8PSK increases much faster (in function of I_{in}^R) than the one obtained for 16QAM. This is because, in the first case, the average variance $\bar{v}$ decreases much faster with the input MI (cf. Figure 2). This behavior illustrates well the aforementioned dependence of the function $f_R(\cdot)$ on the LC and the input MI.

Finally, note that thanks to the shown analytical EXIT charts, we may decide which modulation should (or not) be employed when the channel state is given in the studied example. Through simulations, we found that for the decoder used in simulations, $I_{out}^R > 0.9$ guarantees the output BER be lower than 10^{-2} (cf. also [3, Figure 10]). Therefore, assuming this value of BER is required by the applications, it is obvious that 16QAM or 8PSK modulations should not be employed because neither in Gray or anti-Gray case, they are able to produce output MI I_{out}^R greater than 0.9.

5.2. BER evaluation

We have indicated that the analytical EXIT charts may be useful to adapt the modulation and/or coding according to the instantaneous channel state. Of course, in practice, it cannot be done graphically and we would rather rely on the value of the BER predicted from the EXIT charts.

To verify the accuracy of the BER analysis for different values of E_b/N_0, Figure 5 shows BER values obtained by means of the receiver T-MMSE for the channel $\mathbf{H}_0$ using

different modulations. Dashed lines represent analytical results, while continuous lines correspond to the results obtained by actually simulating the transmission. Only the first five iterations are shown for clarity, above that number small improvement of BER was observed.

For the Gray mapping we note that our analytical method is slightly pessimistic and we attribute it to the simplifying assumption (A2) in Section 4. Assuming SNR to be constant in time n, underestimates the value of MI obtained when comparing to the implemented receiver, which *does* handle the time-dependent variance of the noise and interference (cf. (8)). However, the discrepancy does not exceed 0.2 dB.

Quite a different effect may be observed for 16QAM modulation with anti-Gray mapping—the analytical method is too optimistic. As we observed, this happens because the assumption (A1) is violated during the simulations, that is, the decoder's output (receiver's input) LLRs do not follow the assumed Gaussian law. Deterioration of the performance for 16QAM with anti-Gray mapping is well observed, because the receiver's input MI has a strong impact on the performance both through the LC and through the demapper. Nevertheless, the results are still within a reasonable 0.5 dB difference. For QPSK with anti-Gray mapping, these effects seem to neutralize and almost the perfect match is obtained.

Similar results were obtained in various randomly picked channels $\mathbf{H}$. However, to give an idea how well the proposed analysis works on average for different scenarios, we carry out the BER analysis in the Rayleigh-fading channel. We note that unlike the previous example (fixed channel), the averaged performance is now dominated by low-performance channels (high BER), that is, this figure indicates how well the "bad" channels' performance is evaluated. The entries of
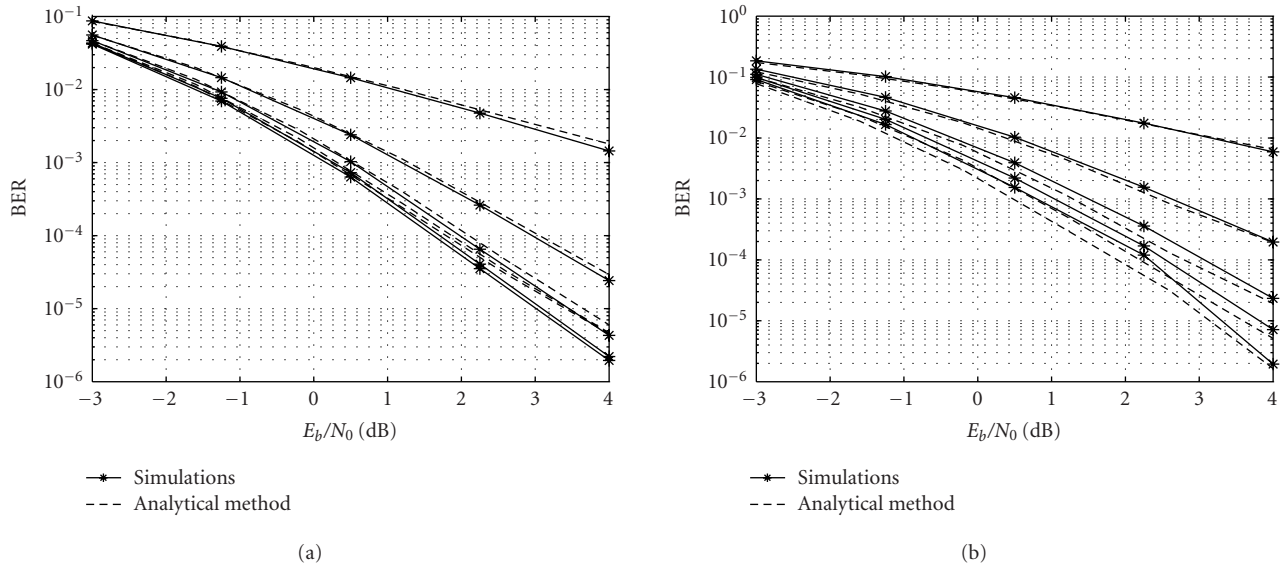
(a)

(b)

FIGURE 6: Simulated and analytical BER obtained by means of T-MMSE receiver in Rayleigh-fading channel **H** for QPSK modulation with (a) Gray mapping and (b) anti-Gray mapping.

the matrix **H** are generated as independent unitary-variance complex Gaussian random variables, so the average E_b/N_0 is defined as $1/B\rho N_0$. The channel is block-fading, that is, constant within a given transmission but varies independently from one transmission to another. The analytical method we propose is applied in each of the channel realizations (10 000 independent channels were generated) and the obtained BER is averaged. We emphasize that the BER should be averaged and not the trajectories or the transfer functions, because all mappings involved in the evaluation process are nonlinear, thus, do not commute with regard to the expectation/averaging operator [27]. The results obtained through the simulations are compared with the analytical method in Figure 6. We may observe that the proposed method matches precisely, that is, within 0.2–0.4 dB, the results obtained through simulations.

Although the method has proven to be very exact in the studied cases, some limitations should be pointed out. In particular,

(i) the assumption of the LLRs independence may lead to significant errors if short data blocks are used. Then the LLRs become highly correlated while the iterative process progresses, which may cause the trajectory to fall off the EXIT functions, as pointed out in [12]. This affects the accuracy of the performance analysis when iterations advance. However, for the length of block used in the paper (4000 bits) this effect was not meaningful;

(ii) the function $G(\cdot, \cdot)$ is obtained assuming that the outputs $y_k(n)$ are Gaussian which is true in the limit, that is, for large systems. Failure of this assumption to hold may cause noticeable effect already at the first iteration. However, we did not observe this effect during the simulations used in the paper;

(iii) the assumption about the pdf of LLRs at the FE's input (decoder's output) is crucial in ensuring the accuracy of the BER prediction, as it affects the calculation of the symbols' variance and, in anti-Gray case, also the demapper's operation. This is particularly well visible in the case of 16QAM with anti-Gray mapping, as already commented.

6. CONCLUSIONS

In this paper we propose a method to evaluate the performance of turbo receivers with linear front-end. The method relies on the EXIT transfer functions obtained using solely available channel state information. The presented analysis is useful to evaluate the performance of the turbo receiver for each iteration in terms of bit error rate (BER). We show that the performance evaluated using the proposed method closely approaches the results obtained by actually running Monte-Carlo simulations in different channels, modulations, and bit mappings. Such an analytical approach provides a good understanding of the working principles of a turbo receiver and may be used to optimize the structure of the transmitter, that is, to adapt the modulation/coding to the known channel conditions, which is a research topic of growing importance.

The presented method has low complexity as it requires only one 2D and three 1D linear interpolations; additionally, the receiver's $\mathbf{w}_k$ has to be calculated in each iteration.

The proposed method and presented results open interesting research venues such as

(i) analysis of the turbo receivers processing very short data blocks or analysis of the receivers based on hard decisions. For the latter, propositions were already made in [7] but the analysis of hard decisions made at

the outputs of the linear combiners (i.e., on the signals $y_k(n)$) may be an interesting venue,

(ii) analysis of the effect of the channel estimation errors on the performance of turbo receivers [6], especially when iterative channel estimation is implemented [5],

(iii) accurate modelling of the SISO decoder which should lead to increased accuracy of the analysis,

(iv) analysis of time-variant linear receivers, which perform better than their time-invariant counterparts studied in this paper. We are currently studying this solution,

(v) development of the analytical methods for nonlinear FE receivers, which are gaining importance thanks to the low-complexity algorithms, for example, based on sphere decoders [4].

APPENDIX

A. AVERAGE SYMBOL VARIANCE

In this section we detail the derivation of formula (18).

As mentioned in (6), the variance of symbols is a function of the a priori LLRs $\Lambda_{c_{k,l}}^{\mathrm{a}}(n)$, which are independent and have identical pdf given by

$$\psi_\Lambda(\lambda; \sigma_\mathrm{I}^2) = \frac{1}{2}\left[\phi(\lambda|0; \sigma_\mathrm{I}^2) + \phi(\lambda|1; \sigma_\mathrm{I}^2)\right]. \quad (\mathrm{A.1})$$

Then, the average variance is computed as

$$\bar{v}(\sigma_\mathrm{I}^2) = \mathrm{E}\{v_k(n)\}$$

$$= \int \cdots \int_{-\infty}^{\infty} v_k(\lambda_1,\dots,\lambda_B) \prod_{j=1}^{B} \psi_\Lambda(\lambda_j; \sigma_\mathrm{I}^2) d\lambda_1 \cdots d\lambda_B. \quad (\mathrm{A.2})$$

Let $v_k(n) = \omega_k(n) - \vartheta_k(n)$, where

$$\omega_k(n) = \sum_{i=1}^{2^B} |\alpha_i|^2 \mathrm{P}(s_k(n) = \alpha_i), \quad (\mathrm{A.3})$$

$$\vartheta_k(n) = \left| \sum_{i=1}^{2^B} \alpha_i \mathrm{P}(s_k(n) = \alpha_i) \right|^2,$$

then $\bar{v}(\sigma_\mathrm{I}^2) = \bar{\omega}(\sigma_\mathrm{I}^2) - \bar{\vartheta}(\sigma_\mathrm{I}^2)$, and indexing k becomes unnecessary, because all symbols have the same variance. To avoid lengthy derivation, it is sufficient to notice that no bias is given to any particular symbol so $\mathrm{E}\{\mathrm{P}(s_k(n) = \alpha_i)\} = 2^{-B}$, where expectation is taken with respect to $\Lambda_{c_{k,l}}^{\mathrm{a}}(n)$. As a consequence, $\bar{\omega}(\sigma_\mathrm{I}^2) = 1$.

Knowing that

$$\mathrm{P}(s_k(n) = \alpha_i) = \prod_{l=1}^{B} \frac{\exp\{b_{i,l}\Lambda_{c_{k,l}}^{\mathrm{a}}(n)\}}{1 + \exp\{\Lambda_{c_{k,l}}^{\mathrm{a}}(n)\}}, \quad (\mathrm{A.4})$$

where $\alpha_i = \mathsf{M}[b_{i,1},\dots,b_{i,B}]$ [3], $\vartheta_k(n)$ may be developed as

$$\vartheta_k(n) = \sum_{i=1}^{2^B} \sum_{j=1}^{2^B} \alpha_i \alpha_j^* \mathrm{P}(s_k(n) = \alpha_i)\mathrm{P}(s_k(n) = \alpha_j)$$

$$= \sum_{i=1}^{2^B} \sum_{j=1}^{2^B} \alpha_i \alpha_j^* \prod_{l=1}^{B} \frac{e^{b_{i,l}\Lambda_{c_{k,l}}^{\mathrm{a}}(n) + b_{j,l}\Lambda_{c_{k,l}}^{\mathrm{a}}(n)}}{\left(1 + e^{\Lambda_{c_{k,l}}^{\mathrm{a}}(n)}\right)^2}, \quad (\mathrm{A.5})$$

and its average is given by

$$\bar{\vartheta}(\sigma_\mathrm{I}^2) = \mathrm{E}\{\vartheta_k(n)\}$$

$$= \int \cdots \int_{-\infty}^{\infty} \sum_{i=1}^{2^B} \sum_{j=1}^{2^B} \alpha_i \alpha_j^* \prod_{l=1}^{B} \frac{e^{(b_{i,l} + b_{j,l})\lambda_l}}{\left(1 + e^{\lambda_l}\right)^2}$$

$$\times \psi_\Lambda(\lambda_l; \sigma_\mathrm{I}^2) d\lambda_1 \cdots d\lambda_B$$

$$= \sum_{i=1}^{2^B} \sum_{j=1}^{2^B} \alpha_i \alpha_j^* \prod_{l=1}^{B} \int_{-\infty}^{\infty} \frac{e^{(b_{i,l} + b_{j,l})\lambda}}{\left(1 + e^{\lambda}\right)^2} \psi_\Lambda(\lambda; \sigma_\mathrm{I}^2) d\lambda. \quad (\mathrm{A.6})$$

Notice that $e^{2\lambda}/(1 + e^{\lambda})^2 = 1/(1 + e^{-\lambda})^2$ and $\psi_\Lambda(\lambda; \sigma_\mathrm{I}^2) = \psi_\Lambda(-\lambda; \sigma_\mathrm{I}^2)$, so, the integral in (A.6) depends only on the value of $b_{i,l} \oplus b_{j,l}$, where $\oplus$ is logical exclusive-or operation. Including this result into (A.6) and considering that $\bar{v}(\sigma_\mathrm{I}^2) = 1 - \bar{\vartheta}(\sigma_\mathrm{I}^2)$, yields (18).

B. APPROXIMATION OF THE EXIT FUNCTION OF THE DEMAPPER

We want to calculate the output MI $I_{\mathrm{out}}^{\mathrm{R}}$ obtained at the output of the demapper $\mathfrak{M}^{-1}[\cdot]$ assuming that its input is given by

$$y = s + \xi, \quad (\mathrm{B.7})$$

where $\xi \sim \mathcal{N}(0, 1/\Gamma)$, $s = \mathfrak{M}[c_1,\dots,c_B] \in \mathcal{A}$, and where we omit the time n and substream k indexes for brevity of notation. We assume also that the extrinsic LLRs of the lth bit are calculated using the max-log simplification of (9):

$$\Lambda_{c_l}^{\mathrm{ex}} = -\min_{\mathbf{b} \in \mathcal{B}_{[l,1]}} \left\{ \Gamma \cdot |y - \mathfrak{M}[\mathbf{b}]|^2 - \sum_{\substack{j=1 \\ j \neq l}}^{B} b_j \Lambda_{c_j}^{\mathrm{a}} \right\}$$

$$+ \min_{\mathbf{b} \in \mathcal{B}_{[l,0]}} \left\{ \Gamma \cdot |y - \mathfrak{M}[\mathbf{b}]|^2 - \sum_{\substack{j=1 \\ j \neq l}}^{B} b_j \Lambda_{c_j}^{\mathrm{a}} \right\}, \quad (\mathrm{B.8})$$

where $\mathbf{b} = [b_1,\dots,b_B]$.

By $\mathbf{c}_{[l,0]}$, we denote a codeword with the lth bit set to "0," and by $\Lambda_{c_l}^{\mathrm{ex}}(\mathbf{c}_{[l,0]})$ the LLR (B.8) obtained when sending $\mathbf{c}_{[l,0]}$, that is, $s = \mathfrak{M}[\mathbf{c}_{[l,0]}]$.

Consider first the case when $I_{\mathrm{in}}^{\mathrm{R}} = 0$. Because $\Lambda_{c_l}^{\mathrm{a}} \equiv 0$, the result of $\min\{\cdot\}$ operation in (B.8) depends only on the distance between y and the constellation points $\mathfrak{M}[\mathbf{b}]$.

Suppose that $\mathbf{c}_{[l,0]}$ was sent and assume high SINR Γ so that $y \approx \mathsf{M}[\mathbf{c}_{[l,0]}]$, then

$$\arg_{\mathbf{b} \in \mathcal{B}_{[l,0]}} \min \left\{ |y - \mathfrak{M}[\mathbf{b}]|^2 \right\} = \mathbf{c}_{[l,0]},$$

$$\arg_{\mathbf{b} \in \mathcal{B}_{[l,1]}} \min \left\{ |y - \mathfrak{M}[\mathbf{b}]|^2 \right\}$$
$$\simeq \arg_{\mathbf{b} \in \mathcal{B}_{[l,1]}} \min \left\{ |\mathfrak{M}[\mathbf{c}_{[l,0]}] - \mathfrak{M}[\mathbf{b}]|^2 \right\} = \hat{\mathbf{c}}_{[l,0]},$$
(B.9)

where $\hat{\mathbf{c}}_{[l,0]}$ denotes the codeword having the lth bit set to "1" and which gives the constellation symbol $\mathfrak{M}[\hat{\mathbf{c}}_{[l,0]}]$ geometrically closest to the symbol $\mathfrak{M}[\mathbf{c}_{[l,0]}]$.

Using (B.9) and (B.7) in (B.8) gives

$$\Lambda_{c_l}^{\text{ex}}(\mathbf{c}_{[l,0]}) = \Gamma \left(|y - \mathfrak{M}[\mathbf{c}_{[l,0]}]|^2 - |y - \mathfrak{M}[\hat{\mathbf{c}}_{[l,0]}]|^2 \right)$$
$$= -\Gamma |\mathfrak{M}[\mathbf{c}_{[l,0]}] - \mathfrak{M}[\hat{\mathbf{c}}_{[l,0]}]|^2$$
$$+ 2\Gamma \mathfrak{R}\{\xi^* (\mathfrak{M}[\hat{\mathbf{c}}_{[l,0]}] - \mathfrak{M}[\mathbf{c}_{[l,0]}])\},$$
(B.10)

where $\mathfrak{R}\{\cdot\}$ denotes the real part. For complex, circularly symmetric ξ (i.e., $\mathrm{E}[\xi\xi] = 0$), the LLR $\Lambda_{c_l}^{\text{ex}}(\mathbf{c}_{[l,0]})$ is Gaussian,

$$\Lambda_{c_l}^{\text{ex}}(\mathbf{c}_{[l,0]}) \sim \mathcal{N}\left(-\frac{1}{2}\epsilon(\mathbf{c}_{[l,0]})\Gamma, \epsilon(\mathbf{c}_{[l,0]})\Gamma \right)$$
$$= \phi(\lambda_l | 0; \epsilon(\mathbf{c}_{[l,0]})\Gamma),$$
(B.11)

with parameters depending only on SNR and the doubled squared distance between constellation symbols:

$$\epsilon(\mathbf{c}_{[l,0]}) = 2 |\mathfrak{M}[\mathbf{c}_{[l,0]}] - \mathfrak{M}[\hat{\mathbf{c}}_{[l,0]}]|^2.$$
(B.12)

The pdf of LLR $\Lambda_{c_l}^{\text{ex}}$ (conditioned only on the bit of interest $c_l = 0$)[7] is random because it depends also on the value of other bits in the codeword c_j, $j \neq l$. The nonrandom (marginal) pdf conditioned only on the bit c_l is, therefore, the mixture of Gaussian distributions. There are $B2^{B-1}$ different Gaussian distributions which may be potentially found (2^{B-1} different pdf's for all B bits). In practice, of course, their number is smaller because the number of *different* $\epsilon(\mathbf{b})$ is small (distances between constellation symbols).

Denote by P the number of different values ϵ_p, $p = 1, \dots, P$, which $\epsilon(\mathbf{c}_{[l,0]})$ may take, and by K_p the number of codewords such that $\epsilon(\mathbf{c}_{[l,0]}) = \epsilon_p$. Because the bits are random and equiprobable, $\kappa_p = K_p/(B2^{B-1})$ has the meaning of probability of choosing the codeword $\mathbf{c}$ such that $\epsilon(\mathbf{c}) = \epsilon_p$. Then, the pdf of the LLRs defined for the all the multiplexed bits is given by

$$p_{\Lambda_{c_l}^{\text{ex}} | c}(\lambda | c = b) = \sum_{p=1}^{P} \kappa_p \phi(\lambda | b; \epsilon_p \Gamma) \quad \text{for } b \in \{0, 1\},$$
(B.13)

[7]The distribution conditioned on $c_l = 1$ may be found through the symmetry/consistency conditions [19].

and the MI of the output is calculated as

$$I_{\text{out}}^{\text{R}} = \sum_{p=1}^{P} \kappa_p \cdot f_{\mathrm{I}}(\epsilon_p \Gamma).$$
(B.14)

Finally, we analyze the case when $I_{\text{in}}^{\text{R}} = 1$, and we note that this condition translates into having an absolute a priori knowledge about the bits c_j, $j \neq l$. Repeating the above analysis we find that $\hat{\mathbf{c}}_{[l,0]}$ denotes now the codeword identical to $\mathbf{c}_{[l,0]}$, except for the lth bit [19]. In fact, since only these two symbols will contribute to (B.8), the pdf of the LLRs is *exactly* Gaussian, even when LLRs are calculated using (9), that is, without approximation (B.8).

In the following we give an example showing how to find the values of P, κ_p, and ϵ_p for the 8PSK modulations with Gray mapping, which—for convenience—we show in Figure 7a. We assume that the most significant bit (MSB) of the codeword $\mathbf{c}$ is c_1.

The LLR conditioned on the MSB $c_1 = 0$, is obtained when $[0, 1, 1]$, $[0, 1, 0]$, $[0, 0, 0]$, or $[0, 0, 1]$ are sent. For example, if $\mathbf{c}_{[1,0]} = [0, 1, 1]$ is sent, then $\hat{\mathbf{c}}_{[1,0]} = [1, 1, 1]$ (the closest symbol having "1" as MSB, cf. Figure 7a) and by simple trigonometric equations we obtain $\epsilon(\mathbf{c}_{[1,0]}) = 2[2\sin(\pi/8)]^2 = \epsilon_1 \approx 1.17$. Note also, that independently of the chosen codeword $\mathbf{c} \in \mathcal{B}_{[1,0]}$, $\epsilon(\mathbf{c}) = \epsilon_1$.

The LLR conditioned on the bit $c_2 = 0$ is obtained when $[0, 0, 1]$, $[1, 0, 1]$, $[1, 0, 0]$, or $[0, 0, 0]$ are sent. If $\mathbf{c}_{[2,0]} = [0, 0, 1]$ is sent, then $\hat{\mathbf{c}}_{[2,0]} = [0, 1, 1]$ and $\epsilon(\mathbf{c}_{[2,0]}) = \epsilon_1$. The same result is obtained sending $\mathbf{c}_{[2,0]} = [0, 0, 0]$. On the other hand, if $\mathbf{c}_{[2,0]} = [1, 0, 1]$ is sent, then $\hat{\mathbf{c}}_{[2,0]} = [0, 1, 1]$ and $\epsilon(\mathbf{c}_{[2,1]}) = \epsilon_2 = 4$. Again, sending $\mathbf{c}_{[2,0]} = [1, 0, 0]$ yields the same result. The same values are obtained for the least significant bit c_3. Therefore, there are only $P = 2$ different values of $\epsilon(\mathbf{c}_{[l,0]})$, and to determine κ_p, we note that for the bits c_2 and c_3, half of the codewords produce the value ϵ_1, and half - ϵ_2, while for the bit c_1 all codewords produce value ϵ_1, that is, $K_1 = 4 + 2 + 2$ and $K_2 = 2 + 2$, so $\kappa_1 = 2/3$ and $\kappa_2 = 1/3$.

Analyzing the case of $I_{\text{in}}^{\text{R}} = 1$, in K_1 cases $\hat{\mathbf{c}}_{[l,0]}$ is the same as when $I_{\text{in}}^{\text{R}} = 0$, that is, κ_1 and ϵ_1 are the same as previously found for $I_{\text{in}}^{\text{R}} = 0$. The difference occur for bit c_2 when $\mathbf{c}_{[2,0]} = [1, 0, 1]$ or $\mathbf{c}_{[2,0]} = [1, 0, 0]$ are sent, because then $\hat{\mathbf{c}}_{[2,0]}$ are $[1, 1, 1]$ and $[1, 1, 0]$, respectively, so $\epsilon(\mathbf{c}_{[2,0]}) = 4(1 + 1/\sqrt{2}) \approx 6.82$. The same situation occurs for bit c_3 when sending $\mathbf{c}_{[3,0]} = [0, 1, 0]$ or $\mathbf{c}_{[3,0]} = [0, 0, 0]$.

Similar analysis may be performed straightforwardly in the case of 16QAM with Gray mapping or for arbitrary modulation when $I_{\text{in}}^{\text{R}} = 1$. For the modulation used in this paper, the values of ϵ_p and κ_p are shown in Table 1.

Finally, note that the presented approach gives satisfactory results when the codewords $\hat{\mathbf{c}}_{[l,0]}$ are found without ambiguity for all the codewords $\mathbf{c}_{[l,0]}$, that is, there are no two codewords $\hat{\mathbf{c}}_{[l,0]}^{\text{a}} \neq \hat{\mathbf{c}}_{[l,0]}^{\text{b}}$ such that $|\mathcal{M}[\hat{\mathbf{c}}_{[l,0]}^{\text{a}}] - \mathcal{M}[\mathbf{c}_{[l,0]}]| = |\mathcal{M}[\hat{\mathbf{c}}_{[l,0]}^{\text{b}}] - \mathcal{M}[\mathbf{c}_{[l,0]}]|$. Such ambiguity may occur if anti-Gray mapping is employed (cf. Figure 7b). For example, consider sending $\mathbf{c}_{[1,0]} = [0, 1, 0]$, then $\hat{\mathbf{c}}_{[1,0]}^{\text{a}} = [1, 0, 1]$, $\hat{\mathbf{c}}_{[1,0]}^{\text{b}} = [1, 1, 1]$. In such case, the LLRs cannot be well approximated as Gaussian and numerical simulation (explained in Section 4.2) should be used.
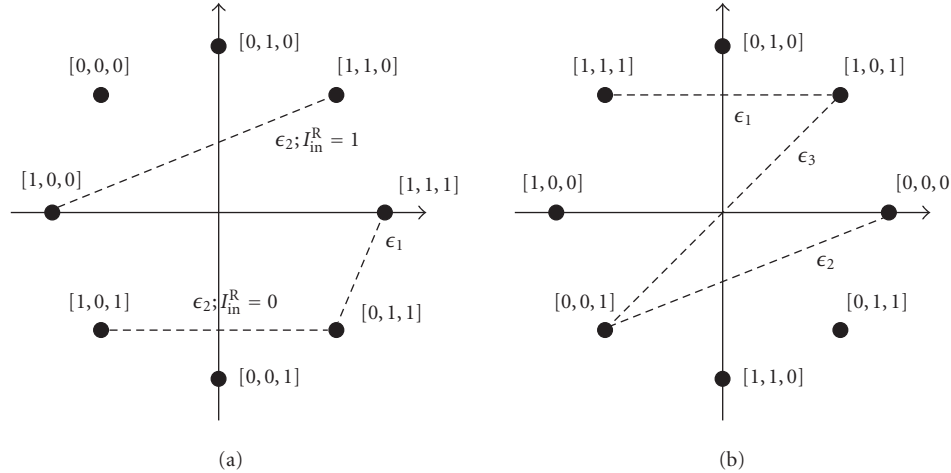
FIGURE 7: Mapping of the codewords **c** into the constellation symbols for (a) 8PSK with Gray mapping, and (b) 8PSK with anti-Gray mapping. The dashed lines, drawn as an example among two symbols only, correspond to the distances used to calculate different values of ϵ_p; for anti-Gray mapping only $I_{in}^R = 1$ is considered.

TABLE 1: Values of the parameters allowing for evaluation of the extrinsic information at the output of the demapper (cf. Section 4.2 and Appendix B).

	BPSK QPSK	Gray mapping				Anti-Gray mapping		
		8PSK		16QAM		QPSK	8PSK	16QAM
I_{in}^R	Any	0	1	0	1	1	1	1
ϵ_1, κ_1	4.0, 1.0	1.17, 0.67	1.17, 0.67	0.8, 0.75	0.8, 0.75	4.0, 0.5	4.0, 0.33	4.0, 0.5
ϵ_2, κ_2	—	4, 0.33	6.82, 0.33	3.2, 0.25	7.2, 0.25	8.0, 0.5	6.82, 0.33	6.4, 0.125
ϵ_3, κ_3	—	—	—	—	—	—	8.0, 0.33	8.0, 0.125
ϵ_4, κ_4	—	—	—	—	—	—	—	10.4, 0.25

REFERENCES

[1] C. Berrou, A. Glavieux, and P. Thitimajshima, "Near Shannon limit error-correcting coding and decoding: Turbo-codes," in *IEEE International Conference on Communications (ICC '93)*, vol. 2, pp. 1064–1070, Geneva, Switzerland, May 1993.

[2] C. Douillard, M. Jézéquel, C. Berrou, A. Picart, P. Didier, and A. Glavieux, "Iterative correction of intersymbol interference: Turbo equalization," *European Transactions on Telecommunications*, vol. 6, no. 5, pp. 507–511, 1995.

[3] M. Tüchler, R. Koetter, and A. C. Singer, "Turbo equalization: principles and new results," *IEEE Trans. Commun.*, vol. 50, no. 5, pp. 754–767, 2002.

[4] B. Hochwald and S. ten Brink, "Achieving near-capacity on a multiple-antenna channel," *IEEE Trans. Commun.*, vol. 51, no. 3, pp. 389–399, 2003.

[5] M. Sellathurai and S. Haykin, "Turbo-BLAST for wireless communications: theory and experiments," *IEEE Trans. Signal Processing*, vol. 50, no. 10, pp. 2538–2546, 2002.

[6] P. D. Alexander, A. J. Grant, and M. C. Reed, "Iterative detection on code-division multiple-access with error control coding," *European Transactions on Telecommunications*, vol. 9, no. 5, pp. 419–426, 1998.

[7] J. Boutros and G. Caire, "Iterative multiuser joint decoding: unified framework and asymptotic analysis," *IEEE Trans. Inform. Theory*, vol. 48, no. 7, pp. 1772–1793, 2002.

[8] X. Wang and H. V. Poor, "Iterative (turbo) soft interference cancellation and decoding for coded CDMA," *IEEE Trans. Commun.*, vol. 47, no. 7, pp. 1046–1061, 1999.

[9] C. Laot, A. Glavieux, and J. Labat, "Turbo equalization: adaptive equalization and channel decoding jointly optimized," *IEEE J. Select. Areas Commun.*, vol. 19, no. 9, pp. 1744–1752, 2001.

[10] M. Tüchler, A. C. Singer, and R. Koetter, "Minimum mean squared error equalization using a priori information," *IEEE Trans. Signal Processing*, vol. 50, no. 3, pp. 673–683, 2002.

[11] T. Richardson and R. Urbanke, "The capacity of low-density parity-check codes under message-passing decoding," *IEEE Trans. Inform. Theory*, vol. 47, no. 2, pp. 599–618, 2001.

[12] S. ten Brink, "Convergence behavior of iteratively decoded parallel concatenated codes," *IEEE Trans. Commun.*, vol. 49, no. 10, pp. 1727–1737, 2001.

[13] H. El Gamal and A. R. Hammons Jr., "Analyzing the turbo decoder using the Gaussian approximation," *IEEE Trans. Inform. Theory*, vol. 47, no. 2, pp. 671–686, 2001.

[14] M. Tüchler, S. ten Brink, and J. Hagenauer, "Measures for tracing convergence of iterative decoding algorithms," in *Proc. 4th International ITG Conference on Source and Channel Coding*, pp. 53–60, Berlin, Germany, January 2002.

[15] G. J. Foschini and M. J. Gans, "On limits of wireless communications in a fading environment when using multiple antennas," *Wireless Personnal Communications*, vol. 6, no. 3, pp. 311–335, 1998.

[16] G. J. Foschini, D. Chizhik, M. J. Gans, C. Papadias, and R. A. Valenzuela, "Analysis and performance of some basic space-time architectures," *IEEE J. Select. Areas Commun.*, vol. 21, no. 3, pp. 303–320, 2003.

[17] X. Li, H. Huang, G. J. Foschini, and R. A. Valenzuela, "Effects of iterative detection and decoding on the performance of BLAST," in *IEEE Global Telecommunications Conference (GLOBECOM '00)*, vol. 2, pp. 1061–1066, San Francisco, Calif, USA, November 2000.

[18] J. G. Proakis, *Digital Communications*, McGraw-Hill, New York, NY, USA, 3rd edition, 1983.

[19] M. Tüchler, "Design of serially concatenated systems depending on the block length," *IEEE Trans. Commun.*, vol. 52, no. 2, pp. 209–218, 2004.

[20] F. Schreckenbach, N. Gortz, J. Hagenauer, and G. Bauch, "Optimization of symbol mappings for bit-interleaved coded modulation with iterative decoding," *IEEE Commun. Lett.*, vol. 7, no. 12, pp. 593–595, 2003.

[21] L. Bahl, J. Cocke, F. Jelinek, and J. Raviv, "Optimal decoding of linear codes for minimizing symbol error rate," *IEEE Trans. Inform. Theory*, vol. 20, no. 2, pp. 284–287, 1974.

[22] D. J. Costello Jr., A. Banerjee, C. He, and P. C. Massey, "A comparison of low complexity turbo-like codes," in *Proc. 36th IEEE Annual Asilomar Conference on Signals, Systems, and Computers*, vol. 1, pp. 16–20, Pacific Grove, Calif, USA, November 2002.

[23] C. Hermosilla and L. Szczecinski, "Turbo receivers for narrow-band MIMO systems," in *Proc. IEEE 28th International Conference on Acoustics, Speech, Signal Processing (ICASSP '03)*, vol. 4, pp. 421–424, Hong Kong, China, April 2003.

[24] M. Sellathurai and S. Haykin, "Turbo-BLAST for high-speed wireless communications," in *Proc. IEEE Wireless Communications and Networking Conference (WCNC '00)*, vol. 1, pp. 315–320, Chicago, Ill, USA, September 2000.

[25] S. Lin and P. S. Yu, "A hybrid ARQ scheme with parity retransmission for error control of satellite channels," *IEEE Trans. Commun.*, vol. 30, no. 7, pp. 1701–1719, 1982.

[26] A. Doufexi, S. Armour, M. Butler, et al., "A comparison of the HIPERLAN/2 and IEEE 802.11a wireless LAN standards," *IEEE Commun. Mag.*, vol. 40, no. 5, pp. 172–180, 2002.

[27] C. Hermosilla and L. Szczecinski, "EXIT charts for turbo receivers in MIMO systems," in *Proc. 7th international Symposium on Signal Processing and Its Applications (ISSPA '03)*, Paris, France, July 2003.

César Hermosilla obtained his B.S. degree in electronic engineering from Technical University Federico Santa María, Chile, in 2000. In 2005, he obtained a Ph.D degree in electronic egineering from the same university. His research interests are in the area of wireless communications, turbo processing, and MIMO systems. He is currently doing a postdoctoral research at INRS Énergie, Matériaux et Télécommunications (INRS-EMT).

Leszek Szczeciński received M.Eng. degree from the Technical University of Warsaw, Poland, in 1992, and Ph.D. degree from INRS-Telecommunications, Canada, in 1997. He held an academic position at the Department of Electrical Engineering, University of Chile, from 1998 to 2000. Since 2001 he has been Professor at INRS-EMT, Montreal, Canada. His research activities are in the area of digital signal processing for telecommunications. He was the Finance Chair of the conference IEEE ICASSP 2004.